Structural modifications of zinc phthalocyanine thin films for organic photovoltaic applications

Structural modifications of zinc phthalocyanine thin films for organic photovoltaic applications

Ying Zhou[1,a)], Tetsuya Taima[1,2 b)], Tetsuhiko Miyadera[2,3], Toshihiro Yamanari[3], Yuji Yoshida[3]

[1]*Research Center of Sustainable Energy and Technology, Kanazawa University, Kakuma, Kanazawa, Japan*

[2]*JST-PRESTO, Japan Science and Technology Agency (JST), 4-1-8 Honcho Kawaguchi, Saitama, Japan*

[3]*Research Center for Photovoltaics, National Institute of Advanced Industrial Science and Technology (AIST), AIST Tsukuba Central 5, 1-1-1 Higashi, Tsukuba, Japan*

Abstract

Zinc phthalocyanine (ZnPc) thin films are vacuum-evaporated on bare indium-tin-oxide (ITO) coated glass by varying substrate temperature and growth rate. The samples are characterized by atomic force microscopy, X-ray diffraction and infrared spectroscopy. The temperature does not play a clear role in the crystalline growth of ZnPc possibly due to the significant structural defects on ITO surface, while it strongly influences the surface morphology and molecular alignment. The relationships between growth characteristics and performances of photovoltaics with planar heterojunction are discussed in detail. Increasing temperature or growth rate leads to a rougher surface morphology, which enables more donor/accepter interface area for photocurrent generation. Moreover, at elevated temperature, more molecules adopt standing-up geometry, resulting in a reduction in overall efficiency. The results imply that low-temperature

[a)] Electronic mail: zhou@se.kanazawa-u.ac.jp, [b)] Electronic mail: taima@se.kanazawa-u.ac.jp

process in order to control the molecular alignment is preferred for efficient organic photovoltaics. By simply increasing the growth rate of ZnPc up to 40 Å/s at room temperature, ZnPc/C60 planar heterojunction shows an efficiency of 1.66%, compared to 1.24% for the cell when ZnPc is prepared at 0.10 Å/s.

I. INTRODUCTION

Organic photovoltaic (OPV) cells using small molecules have been regarded as a potentially useful source of renewable energy due to their important advantages including low weight, low cost and flexibility.[1] Significant progresses have been achieved in OPV since the introduction of donor-acceptor (DA) interface.[2] In this structure, photogenerated excitons in donor or acceptor diffuse to the DA interface where charge dissociation occurs, resulting in generation of free holes and electrons. Power conversion efficiency (PCE) of such devices is strongly limited by several instinct factors including light absorption, exciton diffusion, charge transfer, and charge collection efficiencies.[3] Especially, the photocurrent is only contributed from the excitons generated within the exciton diffusion length from the DA interface. This phenomenon limits the active organic layer thickness, and thus reduces the absorption efficiency. There are usually two possible techniques to overcome the limitation: preparing bulk heterojunction by

co-evaporating two materials to form a blend film; optimizing the thickness, molecular order and the morphology of organic materials.[4,5] In order to modify the structures of bulk heterojunction, controlling the growth condition[6-8] or introduction of buffer layers[9,10] has been investigated. High PCEs of 5-6% for single OPV cell have been reported.[11,12] On the other hand, planar heterojunction with desired morphology and crystalline order is also expected to achieve efficient OPV. Especially, the biggest advantage of vacuum evaporation is the control on the structure and thickness of organic films. It has been reported that the nano-scale multilayer heterojunction with ultrathin crystalline organic films can greatly improve photocurrent genration.[13,14]

As one of the most promising OPV materials, metal phthalocynine including zinc phthalocyanine (ZnPc) is attracting continual interests due to its high absorption coefficient and good chemical and thermal stability.[15] The growth characteristics of evaporated phthalocynine films have been experimentally and theoretically investigated. In most of literatures, phthalocynine films were prepared on clean substrates such as the single-crystal substrate and glass.[16-18] However, for OPV applications, the indium-tin-oxide (ITO) coated glass which has significant structural defects is usually used as a substrate. Understanding the growth of organic thin films on the ITO surface is becoming crucial for further improving OPV cells. This paper focuses the relationship between growth characteristics of ZnPc and the photovoltaic properties.

The growth conditions were varied to modify the structures of ZnPc thin films. Then, fullerene (C60) was deposited to fabricate ZnPc/C60 planar heterojunction. The results indicate that cell performances are strongly dependent on the morphology and molecular alignment of ZnPc films. Although similar fill factor (FF) values of above 0.56 are achieved in all cells, the PCE varies from 0.68 to 1.10%. With considerations of some important factors including surface morphology, crystalline order and molecular alignment that determine the performances, low-temperature process is proposed for efficient ZnPc-based OPV cells.

II. EXPERIMENTAL

Commercial ITO was treated with oxygen plasma for 30 minutes before use. ZnPc was further purified three times. ZnPc thin films were grown in an ultra-high-vacuum (UHV) evaporation system under a deposition pressure of about 1×10^{-6} Pa. A quartz-crystal oscillation was used to monitor the thickness and growth rate, which were verified by Dektak 8 surface profiler (Veeco). The substrate temperature was varied from room temperature (25 ± 1 ^{o}C) to 150 ^{o}C, when growth rate was kept at 0.10 ± 0.05 Å/s. Growth rate was varied as 0.02 ± 0.02, 0.10 ± 0.05, 0.20 ± 0.05 and 0.40 ± 0.10 Å/s. To avoid the structural variations in C60 films, after deposition of ZnPc films, C60 film, LiF (0.1 nm) and Al (100 nm) were deposited, respectively on more than 4 different substrates at one time. The cell area was 0.04 cm^2. The

current density versus voltage (*J-V*) characteristics of the cells were measured under dark and simulated AM 1.5G solar illumination with a Keithley 2400 Digital Source Meter. Incident power was calibrated by using a standard cell to match 1-sun intensity (100 mW/cm^2). Incident photon-to-electron conversion efficiency (IPCE) spectra were collected by using a Xe lamp, which was integrated with a computer controlled monochromater. Source power spectrum was measured by using a calibrated silicon photodiode. Surface morphology was investigated with atomic force microscopic (AFM, SII) in dynamic mode. Crystalline order was measured with X-ray diffraction (XRD) in Bragg-Brentano configuration by using a 9 kW rotating anode generator (Rigaku). The molecular alignment was in-situ monitored with polarized infrared reflection absorption spectroscopy (FTIR-RAS, JASCO) spectrometer at an incidence angle of 80^o. IR data collection consisted of 1024 scans of background and samples. The photoemission spectroscopy of ZnPc film was collected at room temperature under N_2 atmosphere (without exposing the samples to air) to estimate its ionization potential.

III. RESULTS AND DISCUSSION

Figure 1 shows the chemical structures of ZnPc and C60, diagram of cell structure and surface morphology of ITO substrate. The growth characteristics of ZnPc thin films on ITO are investigated in detail. ~~The current-density-voltage (*J-V*) curves of ZnPc (20 nm)/C60 (80 nm)~~

planar heterojunctions under 1 sun are given in Fig. 2. Clearly, the cells using ZnPc grown at 25 and 110 °C show the best performances. The detailed relationship between temperature and the OPV characteristics including the PCE, open-circuit voltage (V_{OC}), short-circuit current density (J_{SC}) and FF are given in Fig. 3. Here, in order to verify the uncertainty, at least 4 cells were fabricated at same growth condition. The relatively poor J_{SC} and V_{OC} are attributed to the thick C60 layer.[19,20] Thick C60 was used to avoid the possibility of leak current. However, thick layer also results in a longer transport distance and reduced minimum carrier density, hence reduced overall efficiency. It is seen that the cell performances are strongly dependent on the temperature of ZnPc films. Note that the cell using ZnPc grown at 25 °C exhibits a PCE of 0.98 ± 0.05%, while slightly increasing the temperature to 50 °C leads to a significant drop in PCE (0.68 ± 0.04%). On the other hand, for the ZnPc grown on heated substrate, the cell performances including PCE, J_{SC} and V_{OC} are increased with temperature up to 110 °C, and then those values drop down at 150 °C. Moreover, all cells exhibit good shape in J-V curves with similar FF values larger than 0.56.

Figure 4 shows the absorption of ZnPc and C60 films, and IPCE curves, which indicates the wavelength dependences of the photocurrent generation efficiency of cell. The IPCE peaks centered at long wavelength region (630 and 700 nm) correspond to the ZnPc absorption (Q-band), while the peak centered at short wavelength region (440 nm) corresponds to C60

~~absorption. The temperature-dependent variations of IPCE in the ZnPc absorption region have an agreement with those of J_{SC}, as shown in Fig. 3(b). The cell using ZnPc grown at 25 °C exhibits the highest efficiencies at above 700 nm, while the cell using ZnPc grown at 110 °C exhibits the highest values in almost Q-band area of ZnPc at below 700 nm. On the other hand, the cell prepared at 25 °C exhibits the lowest IPCE at short wavelength region (C60 absorption), and the efficiency increases with temperature up to 110 °C, and then decreases at 150 °C.~~

~~The variations of the cell performances should be associated with the growth characteristics of ZnPc films.~~ Figure ~~5~~ 2 shows the AFM images of 20 nm ZnPc thin films ~~grown on ITO~~. The ZnPc film prepared at 25 °C exhibits small stick-like grain, while the heated films exhibit round grains with similar size in a range of 40-80 nm. The root-mean-square (RMS) roughness is plotted as a function of growth temperature in Fig. 6. At elevated temperature ranging from 50 to 150 °C, the roughness of ZnPc is approximately lineally increased with temperature. As shown in Fig. 1(c), ITO substrate also exhibits nano-sized round grains with a roughness of 2.1 nm. It implies that the nucleation of ZnPc is strongly dependent on the surface morphology of ITO. ~~The variations in surface morphology of ZnPc prepared at above 50 °C are responsible for the improvements in J_{SC} as well as IPCE. It is known that the rougher surfaces can increase the ZnPc/C60 interface area, which enables more efficient dissociation of excitons into carrier. On the other hand, the presence of voids can also increase the chance of short circuiting, leading to~~

~~an improvement in the charge transport. Thus, J_{SC} is generally increased with surface roughness. Typically, IPCE values at C60 absorption area are enhanced with the surface roughness (temperature) of ZnPc. Note that for the film prepared at 150 °C, most of grains exhibit a height above 30 nm, which is larger than its average thickness (about 20 nm, verified by Dektak surface profiler), indicating a discontinues morphology. The cell using such film (150 °C) shows a small decrease in J_{SC}, while a large decrease in V_{OC} compared with those prepared at 110 °C. Possible reasons for the decreases include large leakage current and direct contact between C60 and ITO electrode due to the very rough surface of ZnPc.[21] On the other hand, the cell using smooth ZnPc prepared 25 °C exhibits the almost highest IPCE in ZnPc absorption area. Moreover, the large drop when ZnPc prepared at 50 °C seems not to result from the surface morphology, because ZnPc films prepared at 25 and 50 °C exhibit close roughness values of 2.33 and 2.43 nm, respectively. Therefore, it is necessary to consider the other factors such as crystalline order and molecular alignment that determine the performances in OPV cells.~~

Figure ~~7~~ 4 shows the XRD results of 20 nm ZnPc films prepared at different temperatures from 25 to 110 °C. There are several peaks centered at 2θ = 21.3°, 30.3° and 35.4°, corresponding to the polycrystalline In_2O_3 (ITO substrate), respectively. The peak centered at 2θ = 6.82° corresponds to a *d* spacing of 12.9 Å, indicating a standing-up crystalline order of ZnPc molecules.[22,23] With increasing the temperature, the peak intensity is slightly increased, while

the peak positions and full width at half maximum (FWHM) are hardly changed. The crystalline domain sizes (crystallite size) are estimated to be 18, 18 and 19 nm, respectively. The result implies that the crystalline order of ZnPc on ITO is not improved by increasing temperature up to 110 ^{o}C.

FTIR-RAS is regarded as a useful method to evaluate the molecular alignment on ITO, because the reflection spectrum of ITO substrate in the region less than 2000 cm^{-1} is similar to highly reflective metal substrate.[24] The spectra were taken at an incidence angle of 80^{o} in *p*-polarization, where the electric field is parallel to the substrate surface. The in-plane variations (lying-down molecular alignment) in the molecules are enhanced in this mode.[25] In Fig. ~~8~~5, there are several absorption peaks related to the vibrations of ZnPc ranging from 700 to 1400 cm^{-1}. The peaks centered at 727, 768 cm^{-1} correspond to the out-of-plane vibrational modes of C-H, while the peak at 752 cm^{-1} and all other peaks at above 800 cm^{-1} correspond to in-plane vibrational modes of ZnPc.[26] Because the vertical vibrations are weakened in *p* polarization mode, the significant out-of-plane peak centered at 727 cm^{-1} indicates that ZnPc molecules being perpendicular (standing-up) on substrate are dominant in all samples, Note that the intensity of such peak is significantly increased with the temperature, while no clear variation can be observed in other peaks. Apparently, more ZnPc molecules adopt standing-up geometry on ITO substrate at elevated temperature, even the temperature is slightly increased to

50 °C. In Fig. ~~6~~4, XRD results indicate the similar crystalline order of these samples. The difference in FITR spectra possibly results from the molecule alignment in amorphous contents or short range order, which is too small to be resolved by XRD. ~~For π-conjugated organic semiconductor, the π-π stacking order is highly expected since it enable better charge transport as well as stronger light absorption,[27] both of which can improve efficiency of photocurrent generation. Comparing with the cell prepared at 25 °C, the large drop in J_{SC} at 50 °C is attributed to the increased content of standing-up ZnPc molecules. In addition, it is known that transfer in molecular alignment always leads to a variation in the absorption spectrum.[22] The shifts in the relative intensities as well as the positions of IPCE peaks at around 630 and 700 nm (Fig. 4) are another evidence that molecular alignment is strongly dependent on growth temperature.~~ Although organic films usually exhibit the polycrystalline or amorphous state on bare ITO substrate, the control of molecular alignment in order to avoid standing-up molecules is feasible and important ~~to achieve efficient photocurrent generation~~. Ionization potential of ZnPc was estimated by photoemission spectroscopy, as shown in Fig. 5. Ionization potential represents the energy difference between HOMO and vacuum level. At higher substrate temperature, the photoelectrons begin emit at smaller phonon energy, indicating a smaller ionization potential. It has been reported that ionization potential is dependent on the molecular alignment, because an intrinsic surface dipole exists in the lying-down molecules, while no such dipole exists in

standing-up molecules.[30] More standing-up ZnPc molecules at higher temperature lead to the shift of ionization potential.

~~Generally, V_{OC} is attributed to the energy offset of the highest occupied molecular orbitals (HOMO) of the donor and the lowest unoccupied molecular orbits (LUMO) of the acceptor. In addition, the carrier loss (i.e. recombination) in charge transport and charge collection processes always leads to a reduction in V_{OC}.[28,29] For example, the offset for ZnPc/C60 heterojunction is around 0.6 eV, while most of ZnPc/C60 OPV cells exhibit a V_{OC} in range of 0.5~0.6 V.[6,8,9,13] Here, the relatively small V_{OC} (0.35~0.47 V) mainly results from the carrier loss in the thick C60 film. To rationalize the relatively larger *Voc* reduction in the cells using ZnPc prepared at 50 and 70 °C, ionization potential of ZnPc was estimated by photoemission spectroscopy, as shown in Fig. 9. Ionization potential represents the energy difference between HOMO and vacuum level. At higher substrate temperature, the photoelectrons begin emit at smaller phonon energy, indicating a smaller ionization potential. It has been reported that ionization potential is dependent on the molecular alignment, because an intrinsic surface dipole exists in the lying-down molecules, while no such dipole exists in standing-up molecules.[30] More standing-up ZnPc molecules at higher temperature lead to the shift of ionization potential. However, the largest difference in ionization potential values is only 0.03 eV, indicating that the molecule alignment has a very small influence on ionization potential. Especially, the cell using ZnPc grown at 110 °C shows~~

~~the largest V_{OC}. All the cells show good shape in J-V curves with similar FF. Thus, the drop in V_{OC} results from neither the HOMO of ZnPc nor a bad FF (i.e. S shaped J-V curves). As shown in Fig. 3, V_{OC} exhibits same temperature dependence with J_{SC}, possibly indicating that the efficiencies in photocurrent generation and charge transport play important roles in both of J_{SC} and V_{OC}. Uhrich *et al.* investigated the effects of hole transport layers on the performances of OPV cells, and pointed out that higher hole mobility can enhance both of J_{SC} and V_{OC}.[31] Possibly more lying-down ZnPc prepared at 25 °C, or rougher surface morphology at elevated temperature, facilities the charge generation and charge transport, which results in higher overall performances.~~

Because of the weak interaction between ITO and ZnPc molecules, Van der Waals forces dominate the nucleation and growth of ZnPc, resulting in standing-up ZnPc molecules.[32] Moreover, as shown in Fig. 1(c), ITO exhibits very rough surface with nano-sized grains ranging from 20 to 40 nm. These significant structural defects suppress the crystalline growth of ZnPc, even the substrate temperature is elevated to 110 °C. It has been reported that smooth ITO substrate or suitable buffer layer enables better control of crystalline order of ZnPc.[33,34] Our results indicate that higher temperature leads to a rougher surface while more standing-up molecules. For π-conjugated organic semiconductor, the π-π stacking order is highly expected since it enable better charge transport as well as stronger light absorption,[27] both of which can

improve efficiency of photocurrent generation. Therefore, low-temperature process is preferred in order to keep a lying-down molecular geometry.

The current density-voltage (*J-V*) curves of ZnPc (20 nm)/C60 (80 nm) planar heterojunctions under 1 sun are given in Fig. ~~2~~6. Clearly, the cells using ZnPc grown at 25 and 110 ^{o}C show the best performances. The detailed relationship between temperature and the OPV characteristics including the PCE, open-circuit voltage (V_{OC}), short-circuit current density (J_{SC}) and FF are given in Fig. ~~3~~7. Here, in order to verify the uncertainty, at least 4 cells were fabricated at same growth condition. ~~The relatively poor J_{SC} and V_{OC} are attributed to the thick C60 layer.[19,20] Thick C60 was used to avoid the possibility of leak current. However, thick layer also results in a longer transport distance and reduced minimum carrier density, hence reduced overall efficiency.~~ It is seen that the cell performances are strongly dependent on the temperature of ZnPc films. Note that the cell using ZnPc grown at 25^{o}C exhibits a PCE of 0.98 ± 0.05%, while slightly increasing the temperature to 50 ^{o}C leads to a significant drop in PCE (0.68 ± 0.04%). On the other hand, for the ZnPc grown on heated substrate, the cell performances including PCE, J_{SC} and V_{OC} are increased with temperature up to 110 ^{o}C, and then those values drop down at 150 ^{o}C. Moreover, all cells exhibit good shape in *J-V* curves with similar FF values larger than 0.56.

Figure ~~4~~8 shows the absorption of ZnPc and C60 films, and IPCE curves, which indicates the

wavelength dependences of the photocurrent generation efficiency of cell. The IPCE peaks centered at long wavelength region (630 and 700 nm) correspond to the ZnPc absorption (Q-band), while the peak centered at short wavelength region (440 nm) corresponds to C60 absorption. The temperature-dependent variations of IPCE in the ZnPc absorption region have an agreement with those of J_{SC}, as shown in Fig. 3(b). The cell using ZnPc grown at 25 ^{o}C exhibits the highest efficiencies at above 700 nm, while the cell using ZnPc grown at 110 ^{o}C exhibits the highest values in almost Q-band area of ZnPc at below 700 nm. On the other hand, the cell prepared at 25 ^{o}C exhibits the lowest IPCE at short wavelength region (C60 absorption), and the efficiency increases with temperature up to 110 ^{o}C, and then decreases at 150 ^{o}C.

The variations in surface morphology of ZnPc prepared at above 50 ^{o}C are responsible for the improvements in J_{SC} as well as IPCE. It is known that the rougher surfaces can increase the ZnPc/C60 interface area, which enables more efficient dissociation of excitons into carrier. On the other hand, the presence of voids can also increase the chance of short circuiting, leading to an improvement in the charge transport. Thus, J_{SC} is generally increased with surface roughness. Typically, IPCE values at C60 absorption area are enhanced with the surface roughness (temperature) of ZnPc. Note that for the film prepared at 150 ^{o}C, most of grains exhibit a height above 30 nm, which is larger than its average thickness (about 20 nm, verified by Dektak surface profiler), indicating a discontinues morphology. The cell using such film (150 ^{o}C) shows

a small decrease in J_{SC}, while a large decrease in V_{OC} compared with those prepared at 110 °C. Possible reasons for the decreases include large leakage current and direct contact between C60 and ITO electrode due to the very rough surface of ZnPc.[21] On the other hand, the cell using smooth ZnPc prepared 25 °C exhibits the almost highest IPCE in ZnPc absorption area. ~~Moreover, the large drop when ZnPc prepared at 50 °C seems not to result from the surface morphology, because ZnPc films prepared at 25 and 50 °C exhibit close roughness values of 2.33 and 2.43 nm, respectively. Therefore, it is necessary to consider the other factors such as crystalline order and molecular alignment that determine the performances in OPV cells.~~ The large drop in J_{SC} at 50 °C is attributed to the increased content of standing-up ZnPc molecules rather than the variation in surface morphology. In addition, it is known that transfer in molecular alignment always leads to a variation in the absorption spectrum.[22] The shifts in the relative intensities as well as the positions of IPCE peaks at around 630 and 700 nm (Fig. 4) are another evidence that molecular alignment is strongly dependent on growth temperature.

Generally, V_{OC} is attributed to the energy offset of the highest occupied molecular orbitals (HOMO) of the donor and the lowest unoccupied molecular orbits (LUMO) of the acceptor. In addition, the carrier loss (i.e. recombination) in charge transport and charge collection processes always leads to a reduction in V_{OC}.[28,29] For example, the offset for ZnPc/C60 heterojunction is around 0.6 eV, while most of ZnPc/C60 OPV cells exhibit a V_{OC} in range of 0.5-0.6 V.[6,8,9,13] To

rationalize the relatively larger *Voc* reduction in the cells using ZnPc prepared at 50 and 70 °C, However, the largest difference in ionization potential values is only 0.03 eV, indicating that the molecule alignment has a very small influence on ionization potential. Especially, the cell using ZnPc grown at 110 °C shows the largest V_{OC}. All the cells show good shape in *J-V* curves with similar FF. Thus, the drop in V_{OC} results from neither the HOMO of ZnPc nor a bad FF (i.e. *S*-shaped *J-V* curves). As shown in Fig. 3, V_{OC} exhibits same temperature-dependence with J_{SC}, possibly indicating that the efficiencies in photocurrent generation and charge transport play important roles in both of J_{SC} and V_{OC}. Uhrich *et al.* investigated the effects of hole transport layers on the performances of OPV cells, and pointed out that higher hole mobility can enhance both of J_{SC} and V_{OC}.[31] Possibly more lying-down ZnPc prepared at 25 °C, or rougher surface morphology at elevated temperature, facilities the charge generation and charge transport, which results in higher overall performances.

~~To verify these considerations,~~ Furthermore, we investigate the effects of growth rate on the performance of OPV cells, where ZnPc (20 nm)/C60 (80 nm) and ZnPc (40 nm)/C60 (50 nm) were fabricated at 25 °C, respectively. The main performances are summarized in Table I. Figure 10(a) shows the PCE of ZnPc (20 nm)/C60 (80 nm) cells and surface roughness of 20 nm ZnPc films as functions of growth rate ranging from 0.02 to 0.40 Å/s. Note that both of PCE and RMS roughness of ZnPc are increased with growth rate. The cell using ZnPc film (RMS: 3.01

nm) prepared at 0.40 Å/s exhibits the highest PCE of 1.10%, which is about 20% larger than that of the cell using heated ZnPc with similar roughness (at 70 ^{o}C, RMS: 3.31 nm). It possibly indicates that larger growth rate also enables a rougher surface with no variation in molecular alignment. As shown in Fig. 10(b), similar improvements are achieved in the ZnPc (40 nm)/C60 (50 nm) cells, which have balanced donor and accepter layers for charge transport. Apparently, control on the growth rate (0.40 Å/s) enhances both of V_{OC} and J_{SC}, resulting in a high PCE of 1.66%.

IV. Conclusions

We have investigated the surface morphology, crystalline order and molecular alignment of ZnPc films on bare ITO substrate by varying the growth conditions. The effects of growth characteristics of ZnPc films on OPV cell performances were discussed in detail. Increasing substrate temperature or growth rate leads to a rougher surface morphology, which enable more donor/accepter interface area for photocurrent generation. On the other hand, increasing the temperature up to 110 ^{o}C cannot enhance the crystalline order of ZnPc, but leads to a clear variation in molecular alignment. Increasing the temperature to 50 ^{o}C leads to significantly more standing-up ZnPc molecules, resulting in a large reduction in overall efficiency of OPV cells. It is obviously that low-temperature process is preferred for fabricating efficient OPV cells, if the

molecular alignment issues of the organic thin films like ZnPc should be considered. By simply increasing the growth rate of ZnPc to 0.40 Å/s at room temperature, ZnPc/C60 planar heterojunction exhibits a power conversion efficiency of 1.66% under 1 sun.

ACKNOWLEDGMENTS

This work was supported by the Precursory Research for Embryonic Science and Technology (PRESTO) program from the Japan Science and Technology Agency (JST).

[1]H. Hoppe and N. S. Sariciftci, J. Mater. Res. **19**, 1924 (2004).

[2]C.W. Tang, Appl. Phys. Lett. **48**, 183 (1996).

[3]P. Heremans, D. Cheyns, and B. P. Rand, Acc. Chem. Res. **42**, 1740 (2009).

[4]S.R. Forrest, MRS Bulletin **30**, 28 (2005).

[5]B.P. Rand, J. Genoe, P. Heremans, and J. Poortmans, Prog. Photovolt: Res. Appl. **15**, 659 (2007).

[6]S. Pfuetzner, J. Meiss, A. Petrich, M. Riede, and K. Leo, Appl. Phy. Lett. **94**, 253303 (2009).

[7]T. Osasa, S. Yamamoto, and M. Matsumura, Adv. Funct. Mater. **17**, 2937 (2007).

[8]S. Pfuetzner, C. Mickel, J. Jankowski, M. Hein, J. Meiss, C. Schuenemann, C. Elschner, A. A. Levin, B. Rellinghaus, K. Leo, and M. Riede, Org. Electron. **12**, 435 (2011).

[9]W. Zeng, K. S. Yong, Z. M. Kam, F. Zhu, and Y. Li, Appl. Phys. Lett. **97**, 133304 (2010).

[10]C. H. Cheng, J. Wang, G. T. Du, S. H. Shi, Z. J. Du, Z. Q. Fan, J. M. Bian, and M. S. Wang, Appl Phys. Lett. 97, 083305 (2010).

[11]F. Yang, M. Shtein, and S. R. Forrest, J. Appl. Phys. **98**, 014906 (2005).

[12]J. Xue, B. P. Rand, S. Uchida, and S. R. Forrest, Adv. Mater. **17**, 66 (2005).

[13]Z. R. Hong, B. Maennig, R. Lessmann, M. Pfeiffer, K. Leo, and P. Simon, Appl. Phys. Lett. **90**, 203505 (2007).

[14]F. Fang, K. Sun, and S. R. Forrest, Adv. Mater., **19**, 4166 (2007).

[15]S. P. Keizer, J. Mack, B. A. Bench, S. M. Gorun, and M. J. Stillman, J. Am. Chem. Soc. **125**, 7067 (2003).

[16]A. A. Zanfolim, D. Volpati, C.A. Olivati, A. E. Job, and C. J. L. Constantino, J. Phys. Chem. C **114**, 12290 (2010).

[17]G. Ricciardi, A. Rosa, and E. J. Baerends, J. Phys. Chem. A **105**, 5242 (2001).

[18]P. Amsalem, L. Giovanelli, J. M. Themlin, and T. Angot, Phys. Rev. B **79**, 235426 (2009).

[19]T. Stubinger and W. Brutting, J. Appl. Phys. **90**, 3632 (2001).

[20]D. Cheyns, J. Poortmans, and P. Heremans, Phys. Rev. B **77,** 165332 (2008).

[21]G. Wei, R. R. Lunt, K. Sun, S. Wang, M. E. Thompson, and S. R. Forrest, Nano Lett. **10**, 3555 (2010).

[22]R. Sathyamoorthy and S. Senthilarasu, J. Electrochem. Soc. **154**, H1 (2007).

[23]T.Sakurai, R. Fukasawa, K. Saito, and K. Akimoto, Org. Electron. **8**, 702 (2007).

[24]M. Tamada, H. Koshikawa, F. Hosoi, and T. Suwa**,** Thin Solid Films **315**, 40 (1998).

[25]A. A. Zanfolim, D. Volpati, C. A. Olivati, A. E. Job, and C. J. L. Constantino, J. Phys. Chem. C **114**, 12290 (2010).

[26]J. S. Louis, D. Lehmann, M. Friedrich, and D. R. T. Zahn, J. Appl. Phys. **101**, 013503 (2007).

[27]C. H. Cheng, J. Wang, G. T. Du, S. H. Shi, Z. J. Du, Z. Q. Fan, J. M. Bian, and M. S. Wang, Appl. Phys. Lett. **97**, 083305 (2010).

[28]W. Tress, K. Leo, and M. Riede, Adv. Funct. Mater. **21**, 2401 (2011).

[29]D. Cheyns, J. Poortmans, P. Heremans, C. Deibel, S. Verlaak, B.P. Rand, and J. Genoe, Phys. Rev. B **77**, 165332 (2008).

[30]S. Duhm, G. Heimel, I. Salzman, H. Glowatzki, R. L. Johnson, A. Vollmer, J. P. Rabe, and N. Koch, Nature Mater. **7**, 326 (2008).

[31]C. Uhrich, D. Wynands, S. Olthof, M. K. Riede, and K. Leo, S. Sonntag, B. Maennig, and M. Pfeiffer, J. Appl. Phys. **104**, 043107 (2008).

[32]W. Chen, D. C. Qi, H. Huang, X. Gao, and A. T. S. Wee, Adv. Funct. Mater. **21**, 410 (2011).

[33]H. Ishihara, T. Kusagaya, S. Tanaka, and I. Hiromitsu, Jpn. J. Appl. Phys. **49**, 081602 (2010).

[34]R. Naito, S. Toyoshima, T. Ohashi, T. Sakurai, and K. Akimoto, Jpn. J. Appl. Phys. **47**, 1416 (2008).

Captions of Figures

FIG. 1. (a) chemical structures of C60 and ZnPc; (b) Diagram of the cell structure; (c) AFM image of ITO patterned glass (scan area: 0.5 × 0.5 μm^2).

FIG. 2. AFM images of ZnPc thin films (scan area: 1 × 1 μm^2) prepared at (a) R.T.; (b) 50 °C; (c) 70 °C; (d) 90 °C; (e) 110 °C, (f) 150 °C. The height is 30 nm for (f).

FIG. 3. Root-mean-square roughness of ZnPc thin films prepared at different temperature.

FIG. 4. XRD patterns of ZnPc thin films prepared at different temperature.

FIG. 5. FTIR-RAS patterns of ZnPc thin films prepared at different temperature.

FIG. 6. Photoemission spectroscopy of ZnPc thin films prepared at different temperature

FIG. ~~2~~7. The *J-V* curves of ZnPc (20 nm)/C60(80 nm) cells using ZnPc prepared at different growth temperature under simulated sunlight.

FIG. ~~3~~8. (a) PCE; (b) V_{OC}; (c) J_{SC}; (d) FF as functions of ZnPc growth temperature. Error bars represent standard deviation.

FIG. ~~4~~9. IPCE spectra of ZnPc (20 nm)/C60(80 nm) OPV cells.

~~FIG. 5. AFM images of ZnPc thin films (scan area: 1 × 1 μm^2) prepared at (a) R.T.; (b) 50 °C; (c) 70 °C; (d) 90 °C; (e) 110 °C, (f) 150 °C. The height is 30 nm for (f).~~

~~FIG. 6. Root-mean-square roughness of ZnPc thin films prepared at different temperature.~~

~~FIG. 7. XRD patterns of ZnPc thin films prepared at different temperature.~~

~~FIG. 8. FTIR-RAS patterns of ZnPc thin films prepared at different temperature.~~

~~FIG. 9. Photoemission spectroscopy of ZnPc thin films prepared at different temperature~~.

FIG. 10. (a) PCE of ZnPc (20 nm)/C60 (80 nm) cells and roughness as functions of ZnPc growth rate. (b) *J-V* curves of ZnPc (40 nm)/C60 (50 nm) cells.

Table I. The performances of ZnPc/C60 cells prepared at 25 ^{o}C.

Cell Structure	Growth Rate (Å/s)	PCE (%)	V_{OC} (V)	J_{SC} (mA/cm^2)	FF
	0.02	0.86	0.40	3.69	0.58
ZnPc (20 nm)/	0.10	0.95	0.41	4.08	0.57
C60 (80 nm)	0.20	1.01	0.44	4.02	0.57
	0.40	1.10	0.44	4.13	0.60
ZnPc(40 nm)/	0.10	1.24	0.50	4.41	0.56
C60 (50 nm)	0.40	1.66	0.53	5.57	0.57

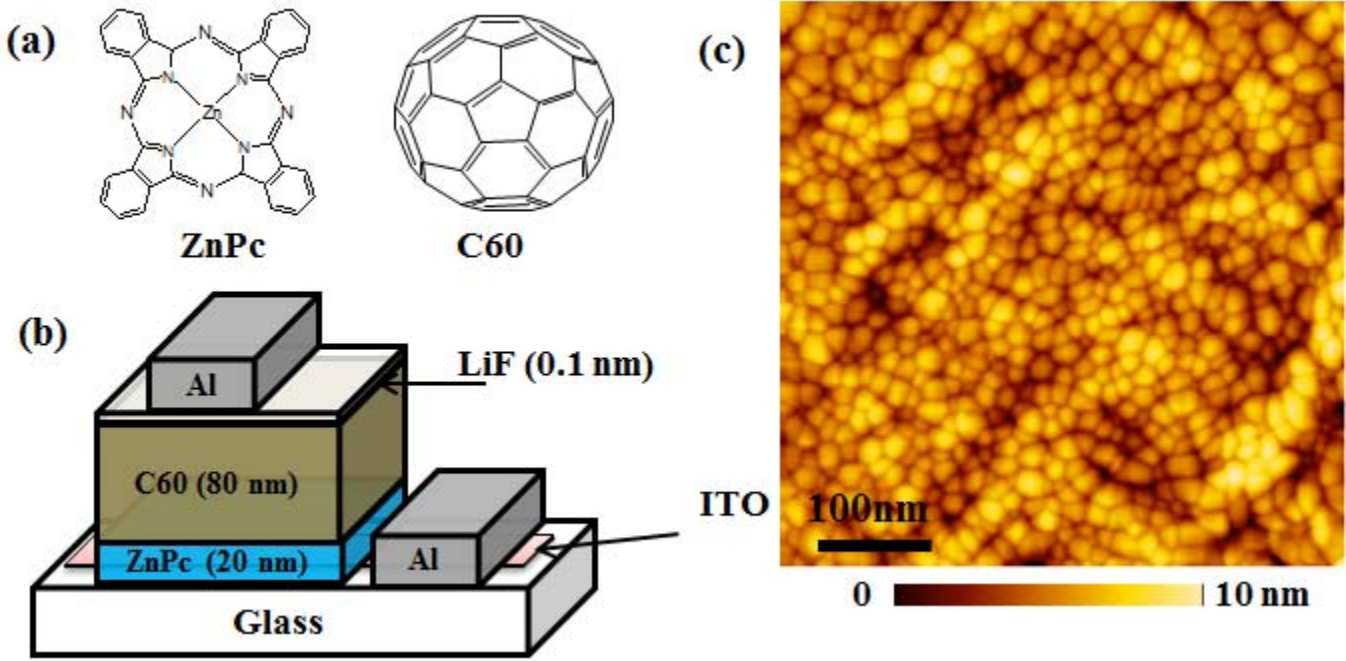
(a)
ZnPc
C60
(b)
Al
LiF (0.1 nm)
C60 (80 nm)
ITO
ZnPc (20 nm)
Al
Glass
(c)
100nm
0
10 nm

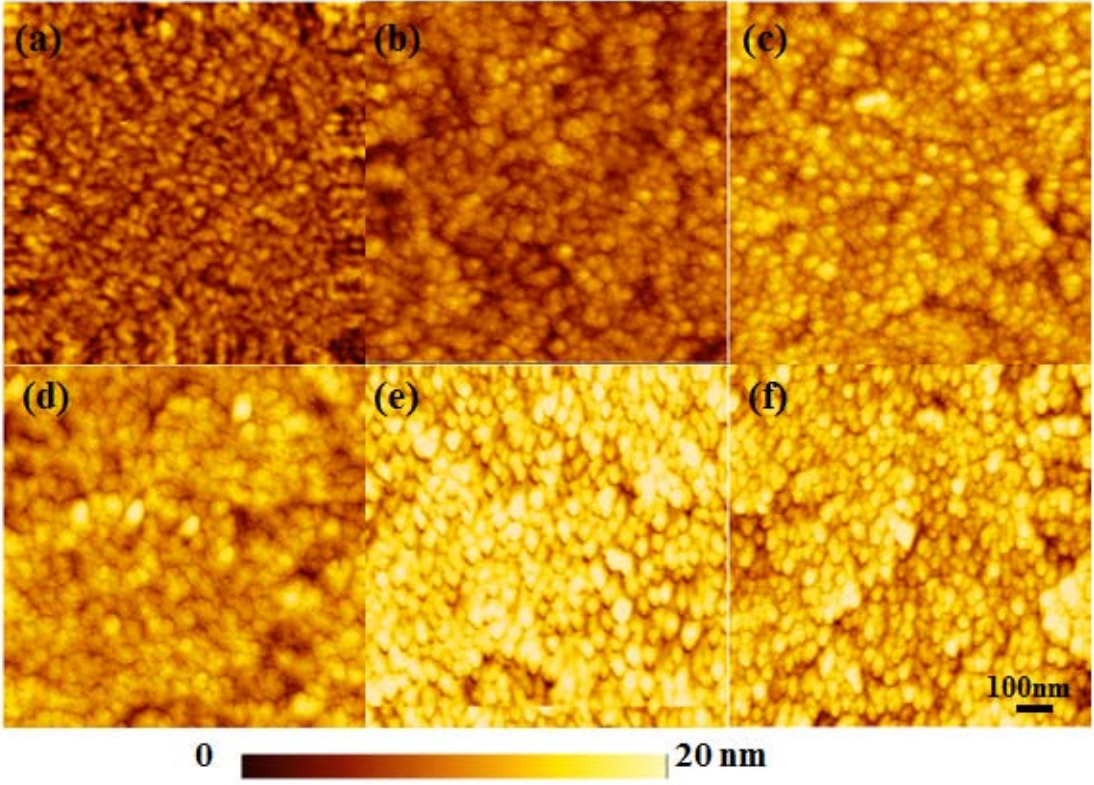
(a)
(b)
(c)
(d)
(e)
(f)
100nm
0
20 nm

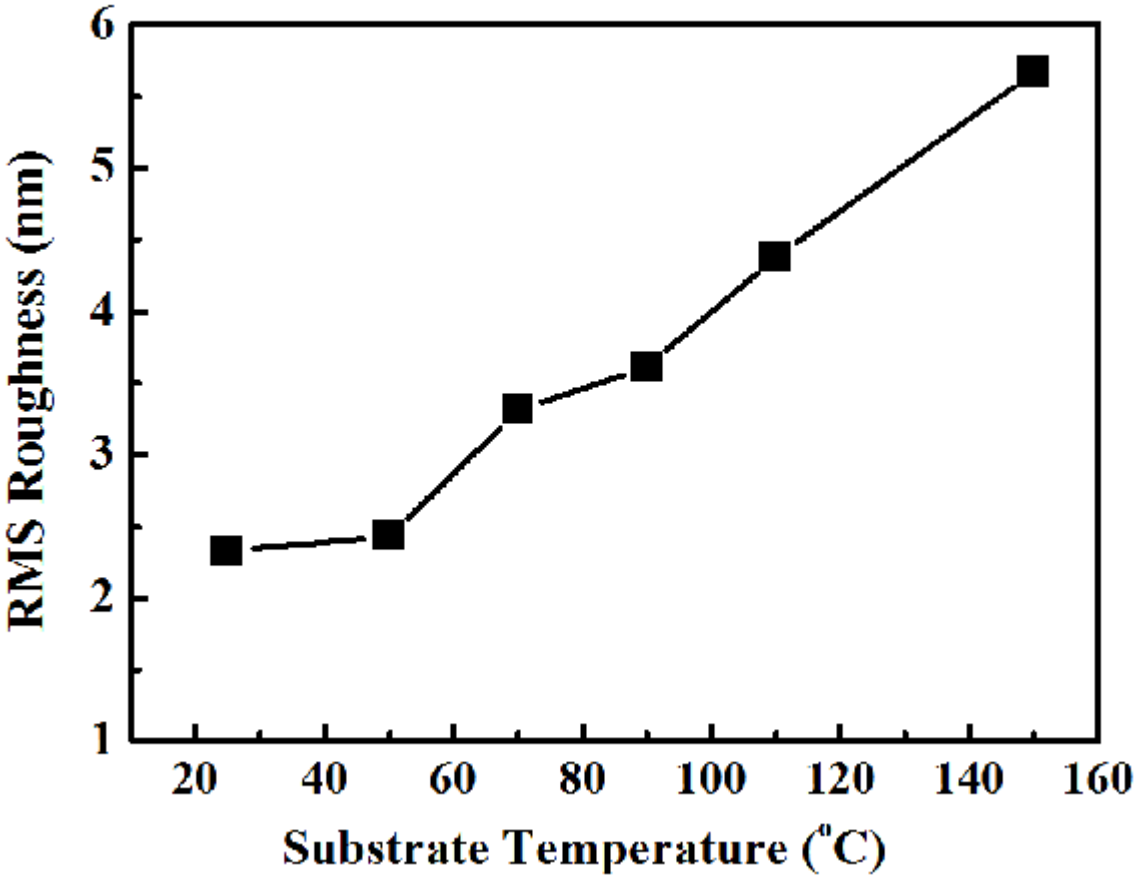
RMS Roughness (nm)
6
5
4
3
2
1
20
40
60
80
100
120
140
160
Substrate Temperature (°C)

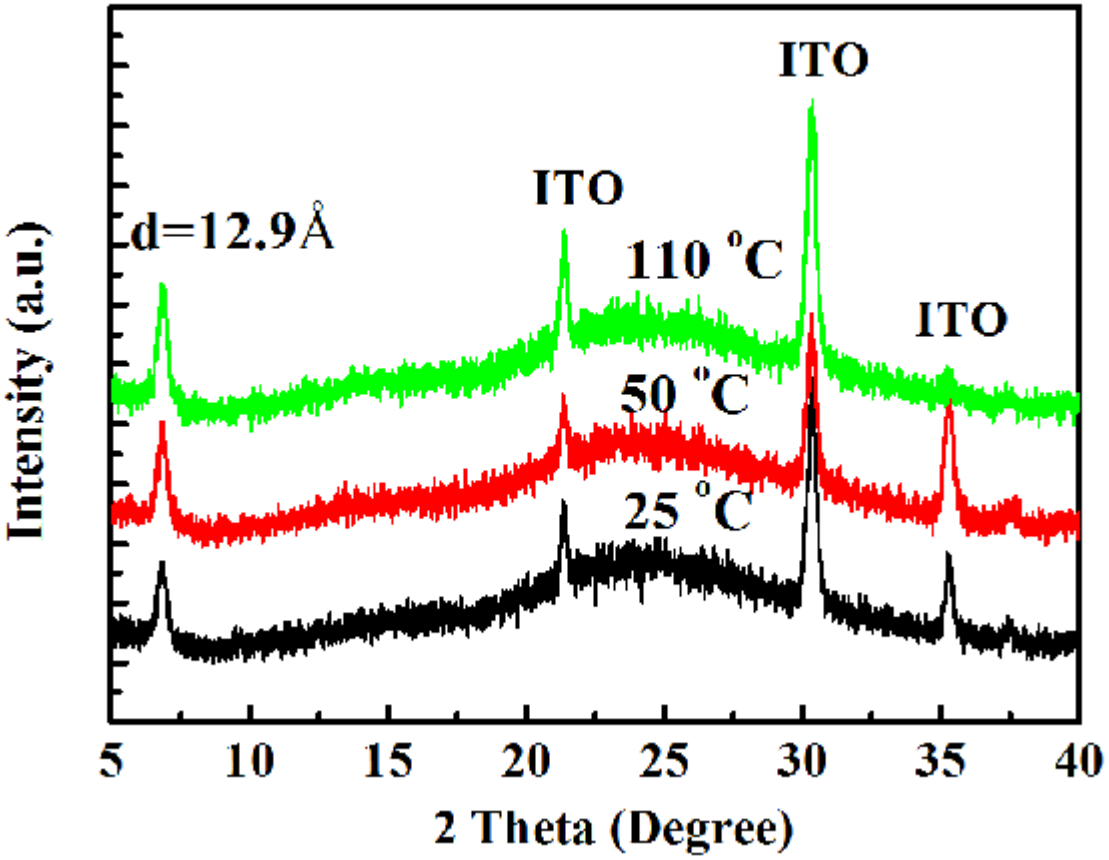
ITO
ITO
d=12.9Å
110 °C
ITO
50 °C
25 °C
Intensity (a.u.)
5
10
15
20
25
30
35
40
2 Theta (Degree)

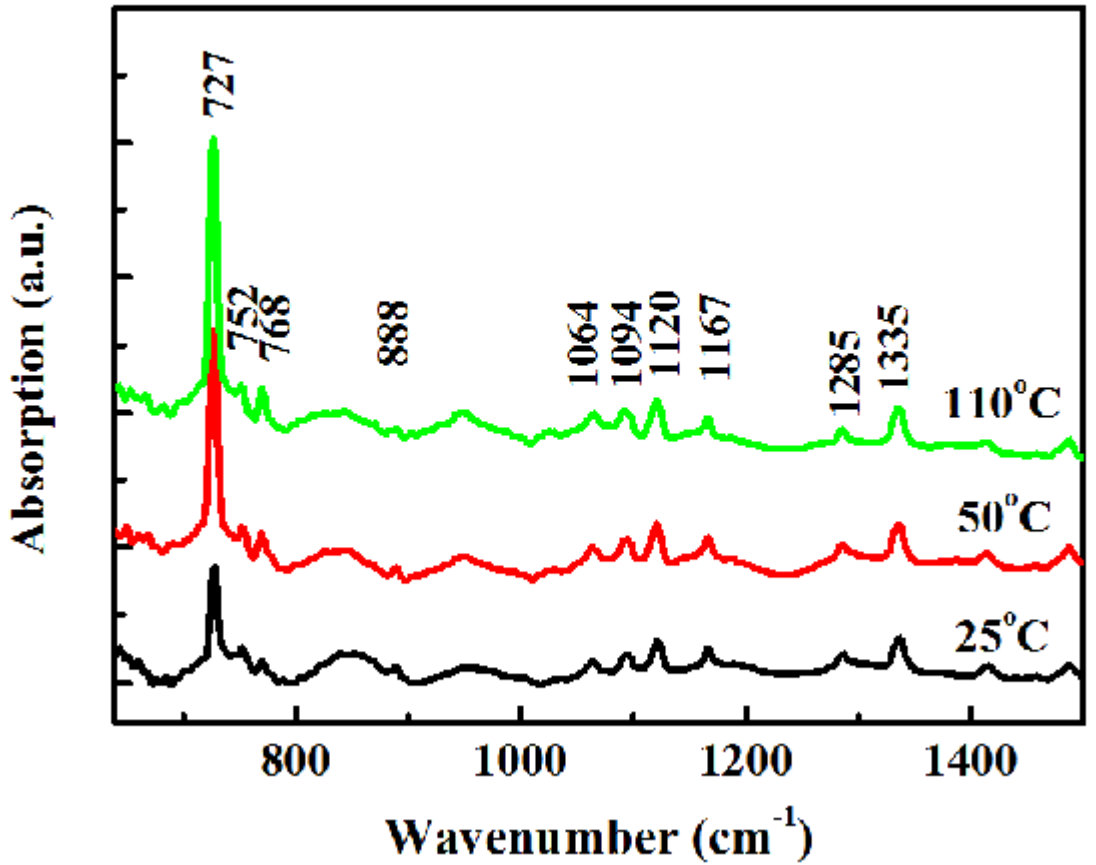
727
752
768
888
1064
1094
1120
1167
1285
1335
110°C
50°C
25°C
Absorption (a.u.)
800
1000
1200
1400
Wavenumber (cm-1)

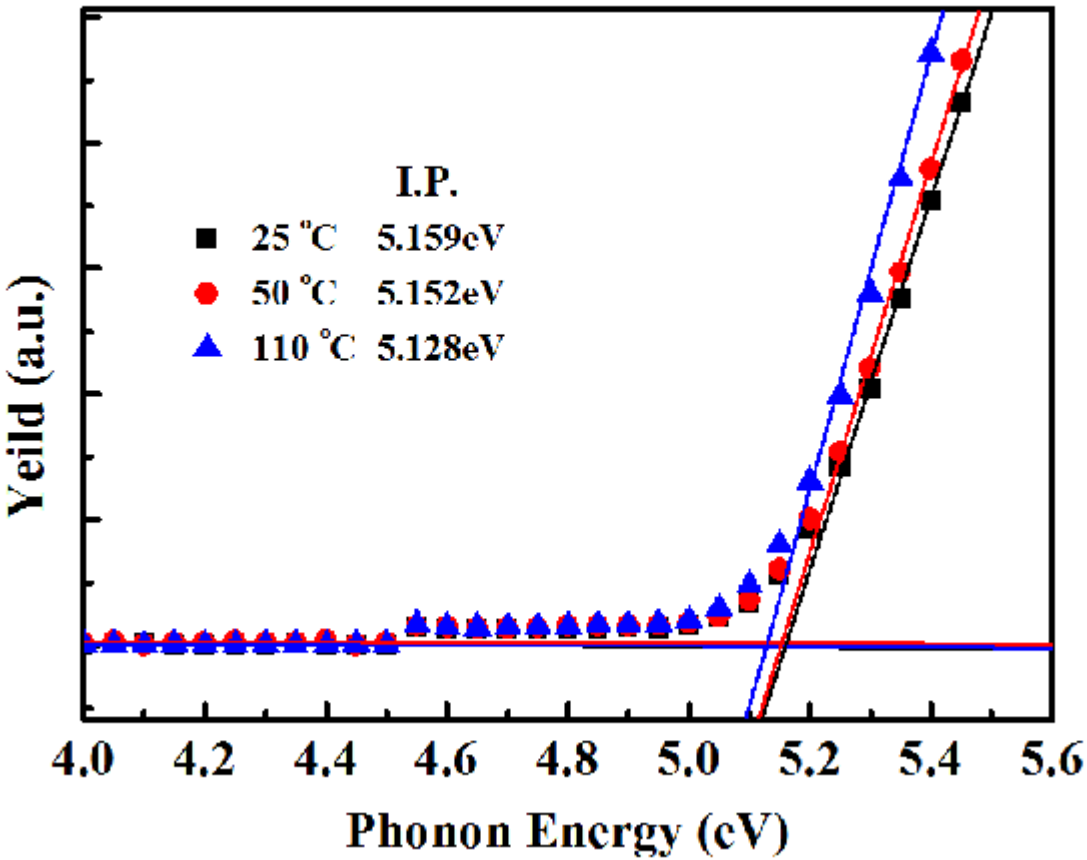
I.P.
25 °C 5.159eV
50 °C 5.152eV
110 °C 5.128eV
Yeild (a.u.)
4.0
4.2
4.4
4.6
4.8
5.0
5.2
5.4
5.6
Phonon Energy (eV)

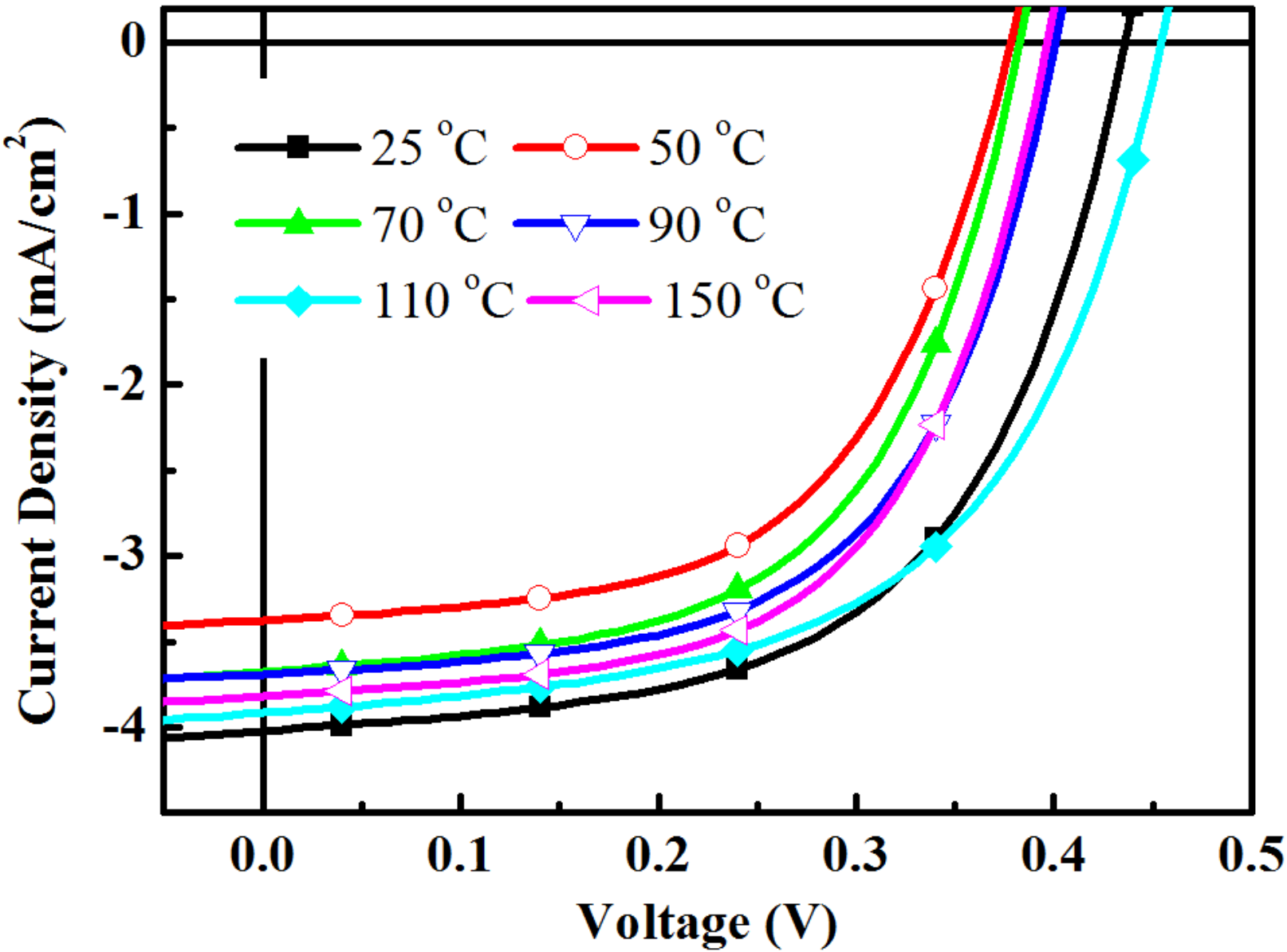
0
-1
-2
-3
-4
Current Density (mA/cm^2)
25 °C
50 °C
70 °C
90 °C
110 °C
150 °C
0.0
0.1
0.2
0.3
0.4
0.5
Voltage (V)

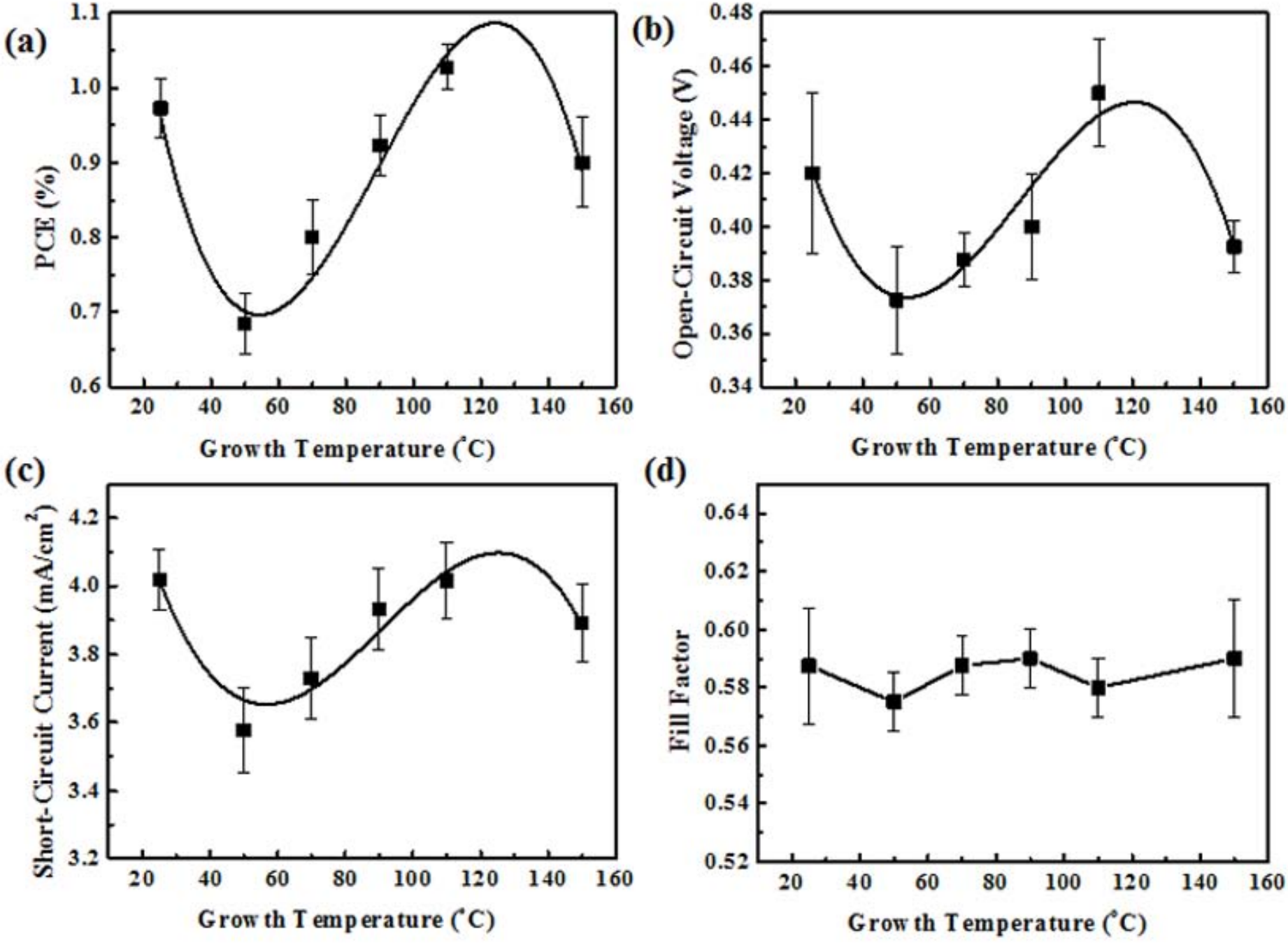
(a)
PCE (%)
Growth Temperature (°C)
(b)
Open-Circuit Voltage (V)
Growth Temperature (°C)
(c)
Short-Circuit Current (mA/cm²)
Growth Temperature (°C)
(d)
Fill Factor
Growth Temperature (°C)

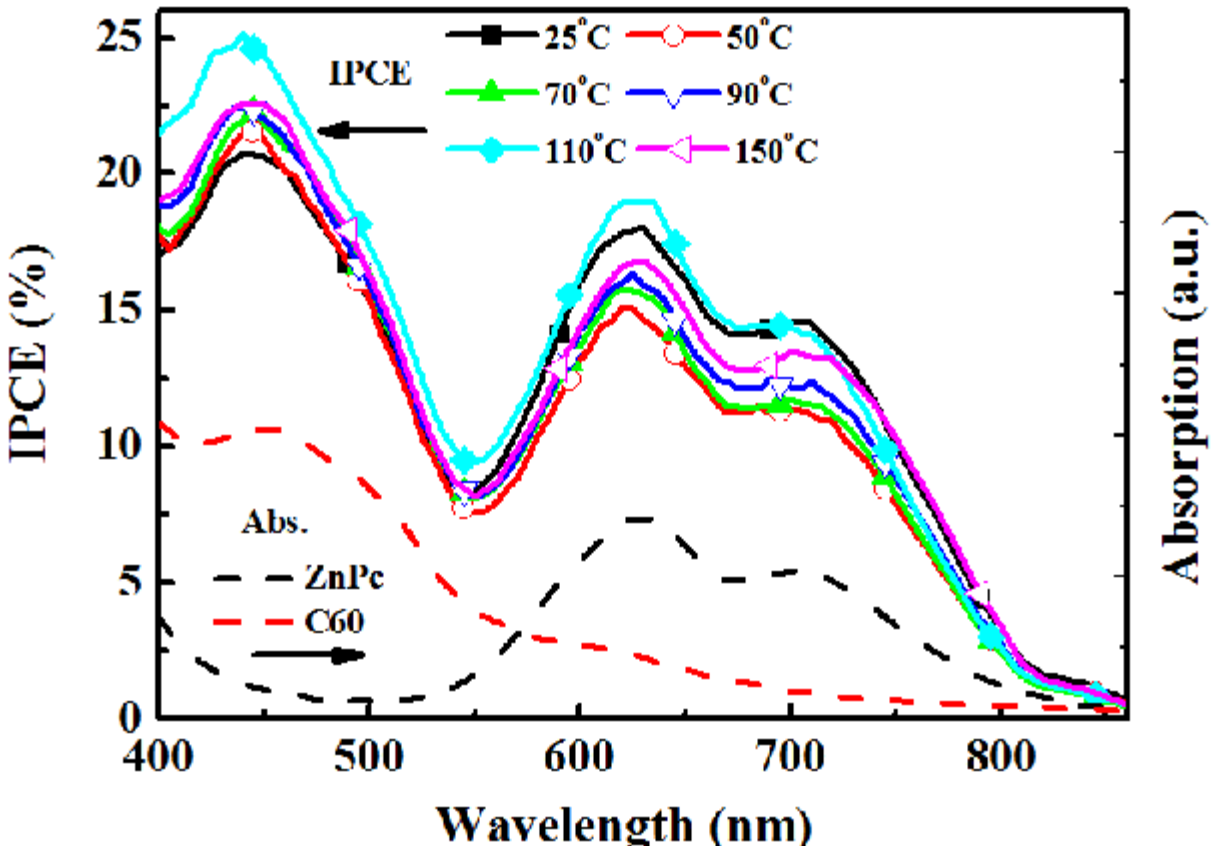
IPCE (%)
Absorption (a.u.)
Wavelength (nm)
IPCE
25°C
50°C
70°C
90°C
110°C
150°C
Abs.
ZnPc
C60
0
5
10
15
20
25
400
500
600
700
800

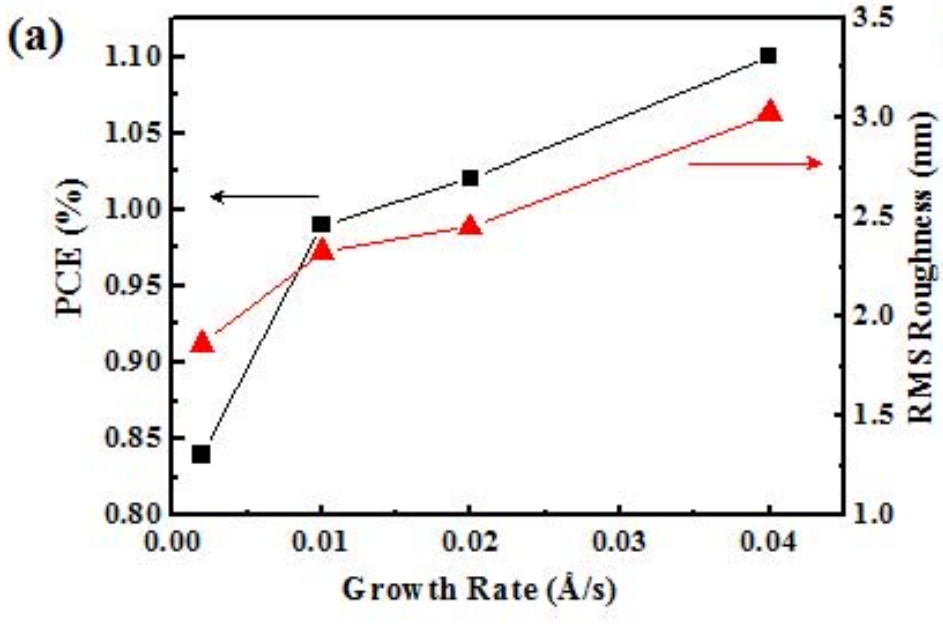
(a)
PCE (%)
RMS Roughness (nm)
Growth Rate (Å/s)
1.10
1.05
1.00
0.95
0.90
0.85
0.80
3.5
3.0
2.5
2.0
1.5
1.0
0.00
0.01
0.02
0.03
0.04

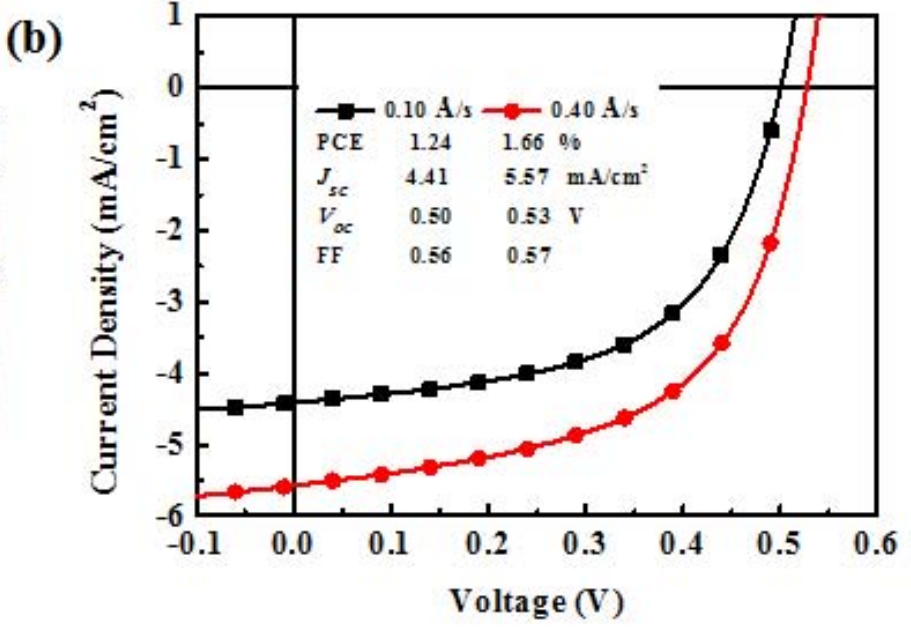
(b)
Current Density (mA/cm^2)
Voltage (V)
0.10 Å/s
0.40 Å/s
PCE 1.24 1.66 %
J_{sc} 4.41 5.57 mA/cm^2
V_{oc} 0.50 0.53 V
FF 0.56 0.57
1
0
-1
-2
-3
-4
-5
-6
-0.1
0.0
0.1
0.2
0.3
0.4
0.5
0.6